

Deep Learning-Assisted Optimal Sensor Placement in Ultrasound NDT

Han Wang¹, Eduardo Pérez^{1,2}, Florian Römer¹

¹ Fraunhofer Institute for Nondestructive Testing IZFP, Saarbrücken, Germany,

² Technische Universität Ilmenau, Ilmenau, Germany
han.wang@izfp.fraunhofer.de

Summary:

In this work we employ model-based deep learning to optimally select the sensing locations of single-channel synthetic aperture measurements in ultrasound nondestructive testing. We use the Fisher information as an optimization target to obtain task-agnostic selection matrices. We then link this result to prior findings on the behavior of the Fisher information matrix.

Keywords: channel selection, deep learning, signal recovery, ultrasound NDT

Background and Motivation

The mutually-related problems of optimal sensor placement and sparse array design are challenging, as they are often non-convex and combinatorial [1]. Recent advances in model-based deep learning have enabled data-driven solutions to these problems. In [1] and [2], soft-max neural networks are employed to achieve the desired structure of a selection matrix while retaining differentiability. Soft-max networks have been successfully applied to MIMO beam pattern design [1], joint optimization of communications and sensing [3], and the subsampling of various multi-channel ultrasound modalities [2].

In our previous work [4], we have analyzed the Cramér-Rao bound (CRB) for target localization in Synthetic Aperture (SA) Ultrasound Nondestructive Testing (UNDT). We highlighted the suitability of the CRB as an optimization target by showing that, in the far-field regime, can be written in terms of properties of the insonification signal and the geometry of the scenario. In this work, we revisit this problem by optimizing the Fisher Information Matrix (FIM). We consider a grid of discrete sensor locations to leverage soft-max neural networks with the goal of choosing the optimal coordinates for the collection of single-channel SA measurements.

Data Model

We consider a 2-D SA scenario with a single scatterer. The transducer is allowed to move along the x-axis. Using a modulated Gaussian pulse as insonification signal, the noiseless amplitude scan (A-scan) measured by placing the transducer at the l^{th} position is modeled in the frequency domain as

$$h(f, \tau_l) = ae^{-\frac{\pi^2}{\beta}(f-f_c)^2 + j(\phi - 2\pi f\tau_l)}, \quad (1)$$

where a is the scattering amplitude, β regulates the bandwidth, f_c and ϕ are the frequency and phase of the carrier, and τ_l is the time delay between the scatterer and the transducer which depends on the coordinates (x, z) of the scatterer.

Sampling (1) over the frequency f , a vector $\mathbf{h}_l \in \mathbb{C}^{N_f}$ is obtained. All L of the noiseless A-scans are then stacked into the vector $\mathbf{h} \in \mathbb{C}^{N_f L}$. In practice, \mathbf{h} can only be observed in the presence of noise. We model the measurement data as $\mathbf{y} = \mathbf{h} + \mathbf{n}$ with $\mathbf{n} \sim \mathcal{CN}(\mathbf{0}, \sigma^2 \mathbf{I}_{N_f L})$, where \mathbf{I}_N is an identity matrix of size $N \times N$. When subsampling \mathbf{y} , only $K \ll L$ A-scans are gathered, which can be represented as

$$\Phi \mathbf{y} = \Phi \mathbf{h} + \hat{\mathbf{n}} \in \mathbb{C}^{N_f K}. \quad (2)$$

In (2), the subsampling matrix Φ has the structure $\Phi = \mathbf{S} \otimes \mathbf{I}_{N_f}$, where $\mathbf{S} \in \mathbb{R}^{K \times L}$ is a selection matrix. Furthermore, \otimes denotes the Kronecker product and the subsampled noise obeys $\hat{\mathbf{n}} \sim \mathcal{CN}(\mathbf{0}, \sigma^2 \mathbf{I}_{N_f K})$.

Proposed Optimization Target

We propose to maximize the elements along the main diagonal of the FIM. This maximizes the sensitivity of the data model to changes in the parameters. However, the FIM is often poorly conditioned, and its trace can be dominated by a small number of parameters that may not be of interest. Let $\xi = [a, x, z]^T$ be a vector containing all the unknown model parameters. The proposed optimization problem is

$$\min_{\xi} \sum_{i \in \mathcal{J}} - \left\| \Phi \frac{\partial \mathbf{h}}{\partial \xi_i} \right\|_2^2 + \lambda \|\Phi \Phi^T - \mathbf{I}_K\|_2^2, \quad (3)$$

where \mathcal{J} is a set containing the indices of the parameters of interest and λ is a hyperparameter. When \mathcal{J} contains all the parameter indices, the first term in (3) is equivalent to the trace.

Simulations

Prior knowledge of the specimen's geometry is available in most NDT applications, which can be used to infer the Region of Interest (ROI). The sensor placement design is optimized such that the image quality in the ROI is prioritized and one can localize critical flaws.

In the pulse echo model (1), the center frequency is $f_c = 4$ MHz and the bandwidth factor is $\beta = f_c^2$. The phase is set as a constant $\phi = -2.6143$. As to the measurements, we utilize $L = 48$ sensor locations with horizontal distance $\Delta x = 0.5$ mm to collect A-scans. Each A-scan consists of $N_f = 46$ Fourier coefficients.

In the simulated scenario, we consider a single point scatterer existing in the specimen. Then, we randomly vary the values of model parameters ξ to generate a training dataset containing 1 million data. The point scatterer locates in the predefined ROI with a higher probability and their scattering amplitudes follow the Gaussian distribution $a \sim \mathcal{N}(15, 3)$.

By importing (3) as the loss function, a soft-max neural network is built to select $K = 24$ optimal sensor locations. The code is implemented in PyTorch and the training process runs on an NVIDIA A100 GPU node.

Results

The Optimal Sensor Placement (OSP) is successfully derived and illustrated in the Fig. 1. In addition, we bring in the Full Sensor Placement (FSP) and Uniform Sensor Placement (USP) for comparison. Because the FSP can serve as a reliable reference and the USP is the easiest sensor placement method to implement in simulation and practice.

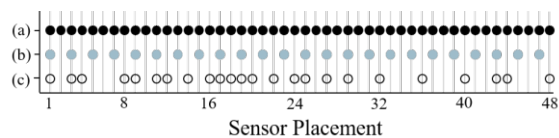


Fig. 1. Sensor placement illustration: (a) Full Sensor Placement (b) Uniform Sensor Placement (c) Optimal Sensor Placement

Furthermore, we apply FISTA to recover the measurement signals that are sampled by the three methods. The three procedures are termed as FISTA + FSP, FISTA + USP and FISTA + OSP, respectively. The reconstructed image quality plays a significant role in the performance evaluation. For further quantitative assessment, we consider the commonly-used Contrast-to-

Noise Ratio (CNR) as the metric, which depends on the correctness of the scatterer's location.

Following the same data generation strategy, we create an evaluation dataset with $N_{\text{Evaluation}} = 1000$. We compute the Cumulative Density Function (CDF) of CNR for the three sensor placement designs and illustrate them in Fig. 2.

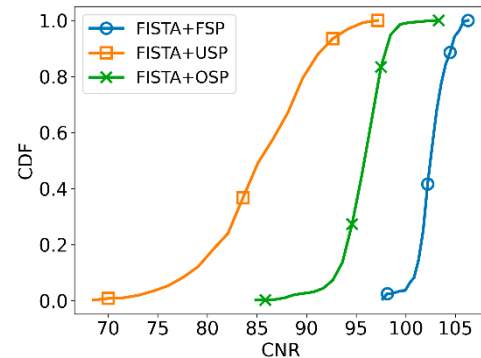


Fig. 2. CDF of CNR for FISTA+FSP, FISTA+USP and FISTA+OSP (right curve indicates a better performance)

By observing the CDF against CNR curves, the right curves indicate a better performance due to a higher CNR of the reconstructed image. Therefore, the image quality of FISTA + OSP is obviously better than FISTA + USP and approaches FISTA + FSP.

Conclusions

This paper demonstrates the application of a soft-max neural network in optimal sensor placement in ultrasound NDT. We take the CRB-related Fisher Information Matrix into account when designing the optimization target. The evaluation results show the feasibility of the optimal spatial subsampling. Furthermore, the algorithm can be applied in sparse array design and be promising in adaptive sensing methods.

References

- [1] K. Diamantaras, Z. Xu, A. Petropulu, Sparse Antenna Array Design for MIMO Radar using Soft-max Selection, (2021)
- [2] I. A. M. Huijben, B. S. Veeling, K. Janse, M. Misch, R. J. G. van Sloun, Learning Sub-Sampling and Signal Recovery with Applications in Ultrasound Imaging, *IEEE Transactions on Medical Imaging* 39(12), 3955-3966 (2020); doi: 10.1109/TMI.2020.3008501
- [3] Z. Xu, F. Liu, A. Petropulu, Cramér-Rao Bound and Antenna Selection Optimization for Dual Radar-Communications Design, *IEEE ICASSP*, 5168-5172 (2022); doi: 10.1109/ICASSP43922.2022.9747651
- [4] E. Pérez, J. Kirchhof, S. Semper, F. Krieg, F. Römer, Cramér-Rao Bounds for Flaw Localization in Subsampled Multistatic Multichannel Ultrasound NDT Data, *IEEE ICASSP*, 2020; doi: 10.1109/ICASSP40776.2020.9053523